Electronic Supplementary Material (ESI) for Dalton Transactions.


# The redox-active Cu-FomA complex: the mode that provides coordination of $Cu^{II}/Cu^{I}$ ions during the reduction/oxidation cycle

Paulina K. Walencik*[a]

## Supplementary Information

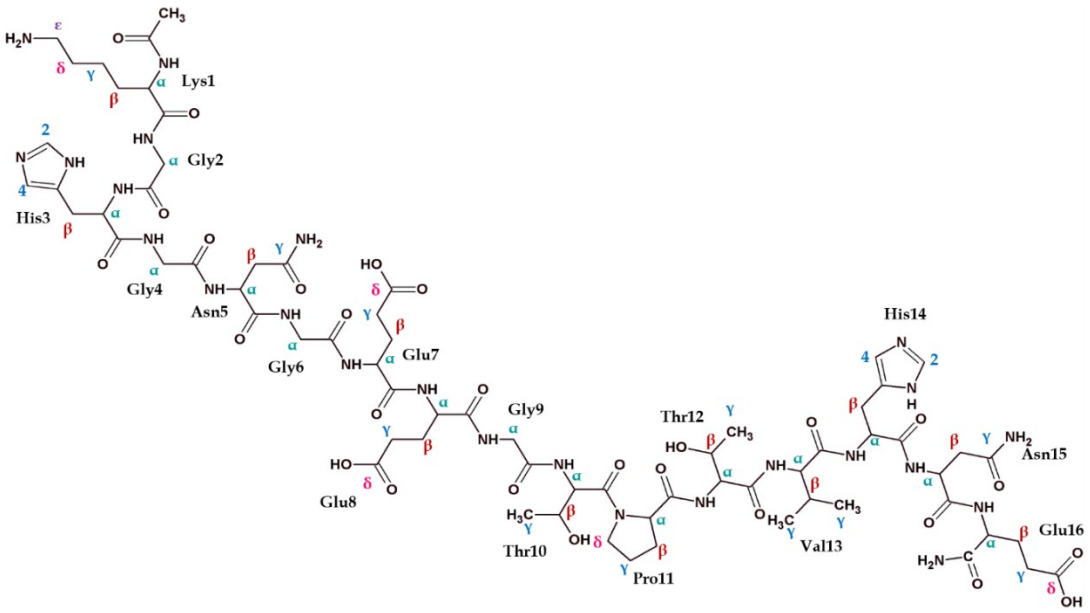


Fig. S1 The primary structure of Fom1 peptide with the NMR proton nomenclature for each amino acid residue. Fom1 sequence: Ac-KGHGNGEEGTPTVHNE-$NH_2$.

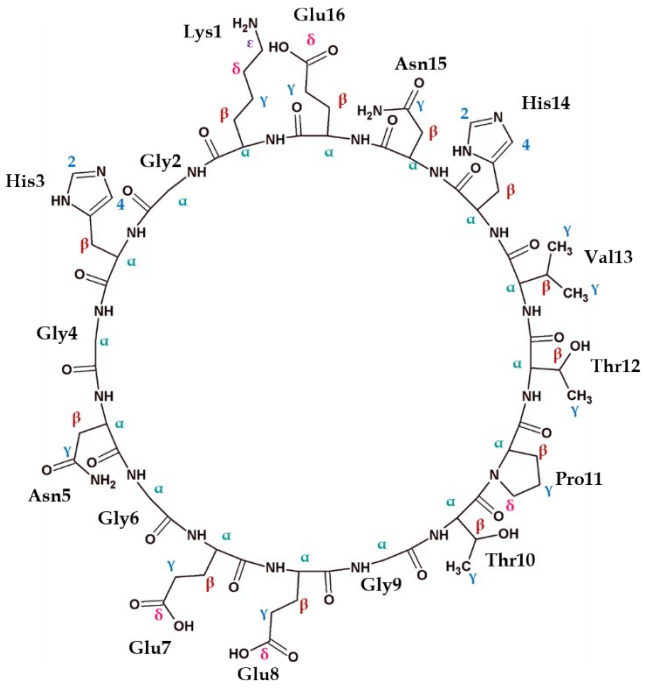


Fig. S2 The primary structure of Fom2 peptide with the NMR proton nomenclature for each amino acid residue. Fom2 sequence: cyclo-(KGHGNGEEGTPTVHNE).

Table S1 $^{1}$H chemical shifts [δ] of Fom1 before and after the addition of 0.8 equivalent of $Cu^{I}$.

| Amino acids residue | $^{1}$H nuclei | δ[ppm] before addition of $Cu^{I}$ | | | δ[ppm] after addition of $Cu^{I}$ | | |
|---|---|---|---|---|---|---|---|
| **Lys1** | Hα | 4.29 | | | 4.28 | | |
| | Hβ | 1.72, 1.82 | | | 1.72, 1.81 | | |
| | Hγ | 1.46 | | | 1.45 | | |
| | Hδ | 1.68 | | | 1.68 | | |
| | Hε | 3.00 | | | 2.99 | | |
| | NH | 8.33 | | | 8.31 | | |
| **Gly2,4,6,9** | Hα | 3.99-3.94 | | | 3.93-3.97 | | |
| | NH | 8.22-8.44 | | | 8.18 | | |
| | | **His3/14** | | **His3/14** | **His3/14** | | **His3/14** |
| **His3,14** | Hα | 4.65 | | 4.65 | 4.21 | | 4.28 |
| | Hβ | 3.03, 3.12 | | 3.01, 3.17 | 3.12, 3.24 | | 3.18, 3.30 |
| | H2 | 7.86 | | 7.89 | 8.04 | | 8.04 |
| | H4 | 7.01 | | 7.03 | 7.09 | | 7.11 |
| | NH | 8.44 | | 7.98 | 8.47 | | 8.31 |
| | | **Asn5/15** | | **Ans5/15** | **Asn5/15** | | **Ans5,15** |
| **Asn5,15** | Hα | 4.54 | | 4.68 | 4.53 | | 4.70 |
| | Hβ | 2.73, 2.87 | | 2.72, 2.80 | 2.72, 2.84 | | 2.72, 2.79 |
| | γ($NH_2$) | | 6.87, 7.59 | | | 6.85, 7.57 | |
| | | | 7.08, 7.60 | | | 7.06, 7.60 | |
| | NH | 8.08 | | 8.04 | 7.95 | | 7.98 |
| | | **Glu7/8/16** | **Glu7/8/16** | **Glu7/8/16** | **Glu7/8/16** | **Glu7/8/16** | **Glu7/8/16** |
| **Glu7,8,16** | Hα | 4.33 | 4.28 | 4.22 | 4.30 | 4.27 | 4.23 |
| | Hβ | 1.93, 2.06 | 1.97, 2.08 | 1.95, 2.09 | 1.93,2.07 | 1.97,2.06 | 1.93,2.07 |
| | Hγ | 2.26 | 2.23 | 2.26 | 2.27 | 2.28 | 2.26 |
| | NH | 8.47 | 8.61 | 8.52 | 8.47 | 8.60 | 8.43 |
| | | **Thr12** | | **Thr10** | **Thr12** | | **Thr10** |
| **Thr10,12** | Hα | 4.30 | | 4.62 | 4.29 | | 4.62 |
| | Hβ | 4.14 | | 4.15 | 4.11 | | 4.16 |
| | Hγ | 1.16 | | 1.25 | 1.11 | | 1.23 |
| | NH | 8.34 | | 8.08 | 8.17 | | 7.91 |
| **Pro11** | Hα | 4.51 | | | 4.45 | | |
| | Hβ | 2.03, 2.33 | | | 2.01, 2.28 | | |
| | Hγ | 1.92 | | | 1.92 | | |
| | Hδ | 3.73, 3.89 | | | 3.74, 3.85 | | |
| **Val13** | Hα | 4.13 | | | 4.10 | | |
| | Hβ | 2.02 | | | 2.01 | | |
| | Hγ | 0.89 | | | 0.88 | | |
| | NH | 8.14 | | | 7.96 | | |
| **C-terminal amide** | $NH_2$ | 7.83, 7.00 | | | 8.03, 7.06 | | |

* δ [ppm] of acetonitrile: 2.09 ppm

Table S2 $^{1}H$ chemical shifts [δ] of Fom2 before and after the addition of 0.8 equivalent of $Cu^{I}$.

| Amino acids residue | $^{1}H$ nuclei | δ[ppm] before addition of $Cu^{I}$ | | | | δ[ppm] after addition of $Cu^{I}$ | | | |
|---|---|---|---|---|---|---|---|---|---|
| **Lys1** | Hα | 4.30 | | | | 4.27 | | | |
| | Hβ | 1.75, 1.85 | | | | 1.70, 1.81 | | | |
| | Hγ | 1.44 | | | | 1.41,1.46 | | | |
| | Hδ | 1.68 | | | | 1.66 | | | |
| | Hε | 3.00 | | | | 2.98 | | | |
| | NH | 8.32 | | | | 8.31 | | | |
| **Gly2,4,6,9** | Hα | 4.04-3.94 | | | | 4.09-3.93 | | | |
| | NH | 8.47-8.22 | | | | 8.52-8.20 | | | |
| **His3,14** | | **His3/14** | | **His3/14** | | **His3/14** | | **His3/14** | |
| | Hα | 4.60 | | 4.66 | | n.d. | | n.d. | |
| | Hβ | 3.05, 3.13 | | 3.04, 3.15 | | 3.18, 3.29 | | 3.18, 3.30 | |
| | H2 | 7.79 | | 7.90 | | 8.01 | | 8.01 | |
| | H4 | 6.99 | | 7.02 | | 7.08 | | 7.12 | |
| | NH | 8.27 | | 8.46 | | 8.30 | | 8.50 | |
| **Asn5,15** | | **Asn5/15** | | **Ans5/15** | | **Asn5/15** | | **Ans5,15** | |
| | Hα | 4.54 | | 4.62 | | 4.52 | | 4.53 | |
| | Hβ | 2.72, 2.86 | | 2.73, 2.86 | | 2.70, 2.85 | | 2.86, 3.02 | |
| | γ($NH_2$) | 6.88, 7.59<br>6.92, 7.60 | | | | 6.86, 7.62<br>6.89, 7.58 | | | |
| | NH | 8.13 | | 8.07 | | 7.95 | | 7.98 | |
| **Glu7,8,16** | | **Glu`7/8/16** | **Glu7/8/16** | **Glu7/8/16** | **Glu7/8/16** | **Glu7/8/16** | **Glu7/8/16** | **Glu7/8/16** | **Glu`7/8/16** |
| | Hα | 4.33 | 4.31 | 4.27 | 4.13 | 4.31 | 4.29 | 4.26 | 4.31 |
| | Hβ | 1.94, 2.08 | 1.94, 2.08 | 1.99, 2.07 | 1.89, 2.03 | 1.93,2.07 | 1.93,2.07 | 2.00,2.07 | 2.07,2.07 |
| | Hγ | 2.27 | 2.25 | 2.28 | 2.19 | 2.27 | 2.25 | 2.28 | 2.28 |
| | NH | 8.46 | 8.34 | 8.59 | 8.01 | 8.43 | 8.33 | 8.61 | 8.57 |
| **Thr10,12** | | **Thr`10/12** | **Thr10/12** | | **Thr10/12** | **Thr10/12** | | **Thr10/12** | **Thr`10/12** |
| | Hα | 4.29/4.50 | 4.37 | | 4.64 | 4.24 | | 4.64 | 4.28 |
| | Hβ | 4.12/4.10 | 4.23 | | 4.18 | 4.13 | | 4.19 | 4.11 |
| | Hγ | 1.17/1.17 | 1.20 | | 1.24 | 1.18 | | 1.23 | 1.10 |
| | NH | 8.35/7.92 | 8.24 | | 7.99 | 8.16 | | 7.90 | 8.17 |
| **Pro11** | Hα | 4.51 | | | | 4.50 | | | |
| | Hβ | 2.03, 2.32 | | | | 2.02, 2.30 | | | |
| | Hγ | 1.94 | | | | 1.95 | | | |
| | Hδ | 3.73, 3.87 | | | | 3.72, 3.87 | | | |
| **Val13** | | **Val`13** | | **Val13** | | **Val13** | | | **Val`13** |
| | Hα | 4.12 | | 4.12 | | 4.06 | | | 4.11 |
| | Hβ | 2.03 | | 2.02 | | 2.00 | | | 2.00 |
| | Hγ | 0.88 | | 0.85 | | 0.85 | | | 0.89 |
| | NH | 8.15 | | 8.03 | | 7.91 | | | 7.95 |

* δ [ppm] of acetonitrile: 2.09 ppm; n.d. – not detected; signals from the second Fom2 conformer has been marked with apostrophe

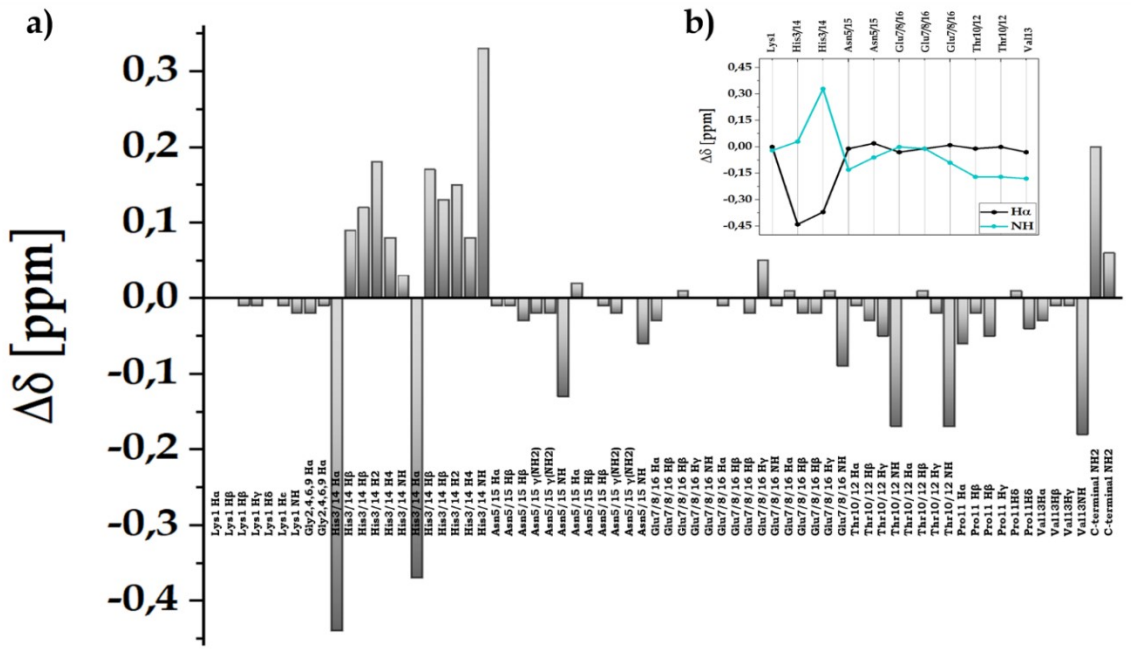


Fig. S3 The chemical shift variations provoked by the $Cu^{I}$ ions on the Fom1 protons. (a) A histogram presenting the measured changes in the values of the chemical shifts ($(\Delta\delta=\delta_{Fom1}-\delta_{Fom1\text{-}CuI})$ for each amino acid residue. (b) A diagram presenting the chemical shift perturbations monitored for the signals of Hα i NH.

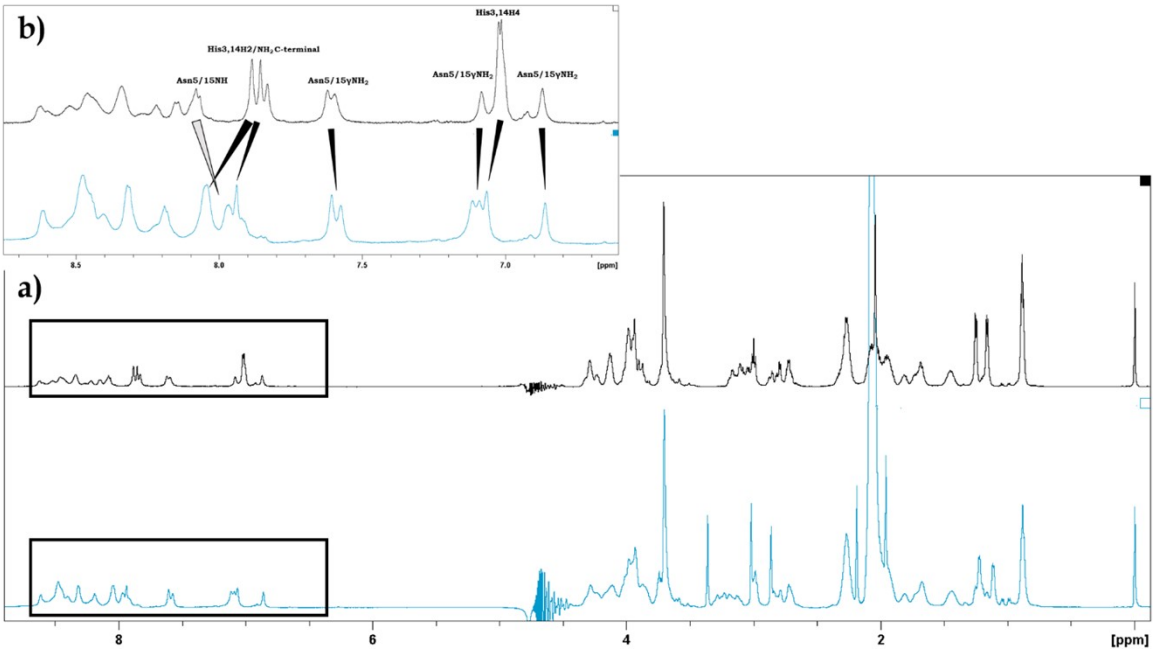


Fig. S4 (a) $^{1}$H-NMR spectra recorded for 4mM Fom1 before (top, black) and after (bottom, blue) the addition of 0.8 equivalents of $Cu^{I}$ ions. (b) The top panel presents a selected region for the aromatic and amide protons. The arrows indicate the most affected protons. Conditions: pH≈ 7.40; 90%$H_2O$/10%$D_2O$, TSP 0.00 ppm. The sample of $Cu^{I}$ complex contained ≈0.5% of MeCN and 3.2 mM of HAsc.

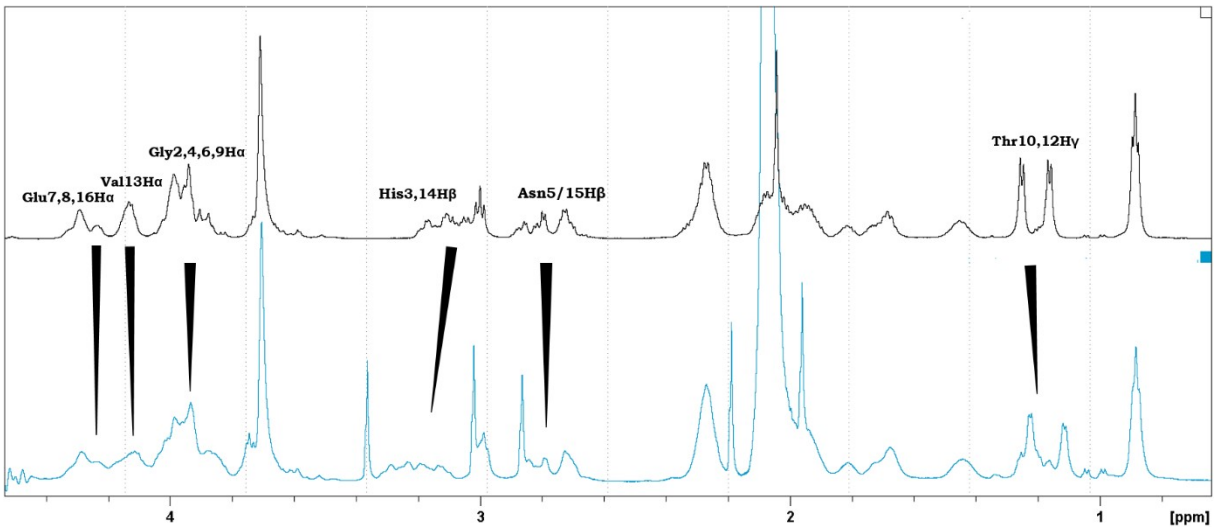


Fig. S5 The $^{1}$H-NMR spectra recorded for 4mM Fom1 before (top, black) and after (bottom, blue) the addition of 0.8 equivalents of $Cu^{I}$ ions with the chosen region for aliphatic protons. The arrows indicate the most affected protons. Conditions: pH≈ 7.40; 90%$H_2O$/10%$D_2O$, TSP 0.00 ppm. The sample of $Cu^{I}$ complex contained ≈0.5% of MeCN and 3.2 mM of HAsc.

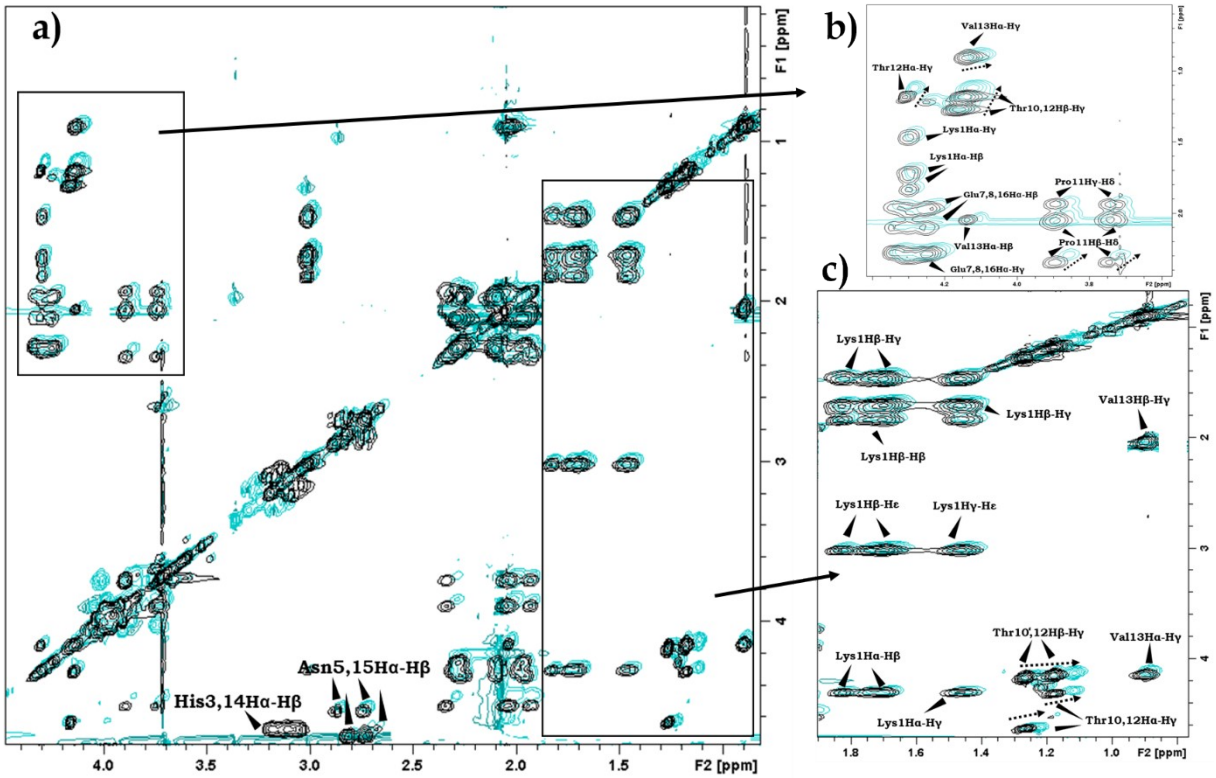


Fig. S6 (a) The $^{1}$H-$^{1}$H TOCSY spectra recorded for 4mM Fom1 before (black) and after (blue) the addition of 0.8 equivalents of $Cu^{I}$ ions with the chosen region for aliphatic protons. (b) and (c) The magnification of selected cross-peaks. The arrows indicate the most affected protons. Conditions: pH≈ 7.40; 90%$H_2O$/10%$D_2O$, TSP 0.00 ppm.

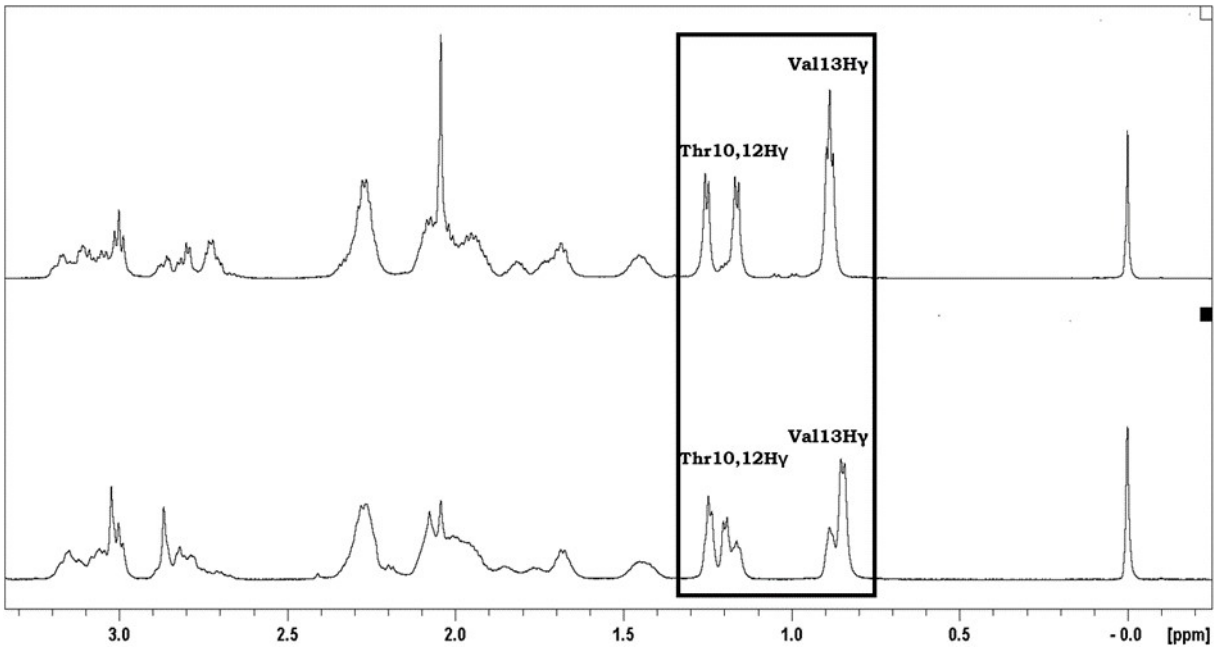


Fig. S7 The comparison of $^{1}$H NMR spectra recorded for Fom1 (top) and Fom2 (bottom) peptides with the chosen region for aliphatic protons. The biggest differences were observed for the Hγ signals of Thr10, Thr12 and Val13 residues indicating the presence of two conformation of Fom2.

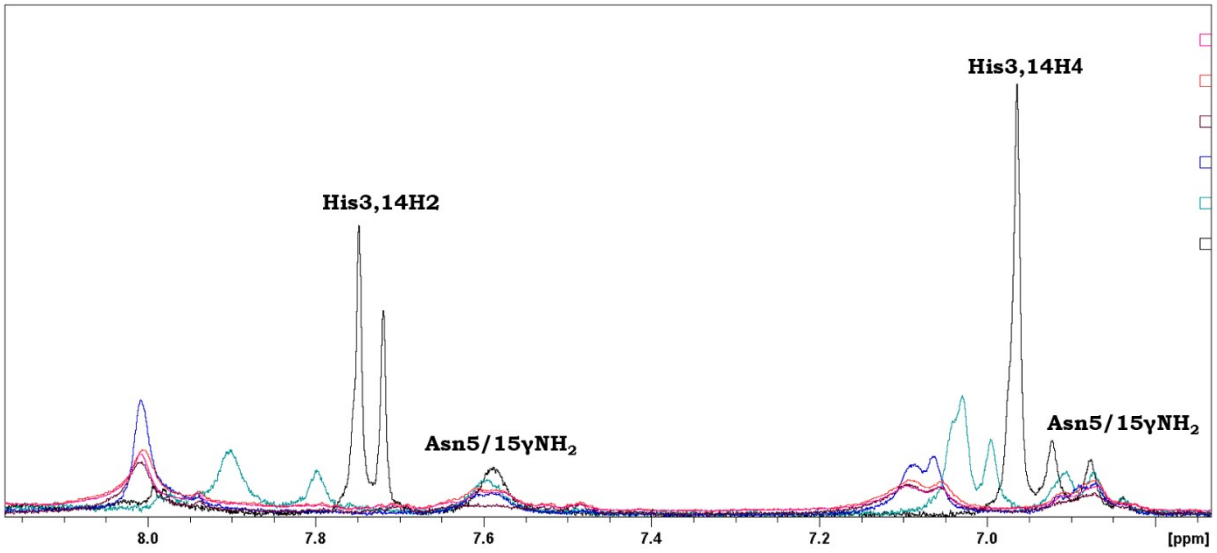


Fig. S8 The selected fragment of the $^{1}$H NMR spectra recorded for Fom2 peptide during the titration experiment: 0 equivalent of $Cu^{I}$ (black), 0.25 equivalent of $Cu^{I}$ (blue), 0.5 equivalent of $Cu^{I}$ (dark blue), 0.8 equivalent of $Cu^{I}$ (red), 1.0 equivalent of $Cu^{I}$ (purple), 1.25 equivalent of $Cu^{I}$ (pink). Conditions: peptide concentration 4mM, pH=7.40; 90% $H_2O$/10% $D_2O$; TSP 0.00 ppm.

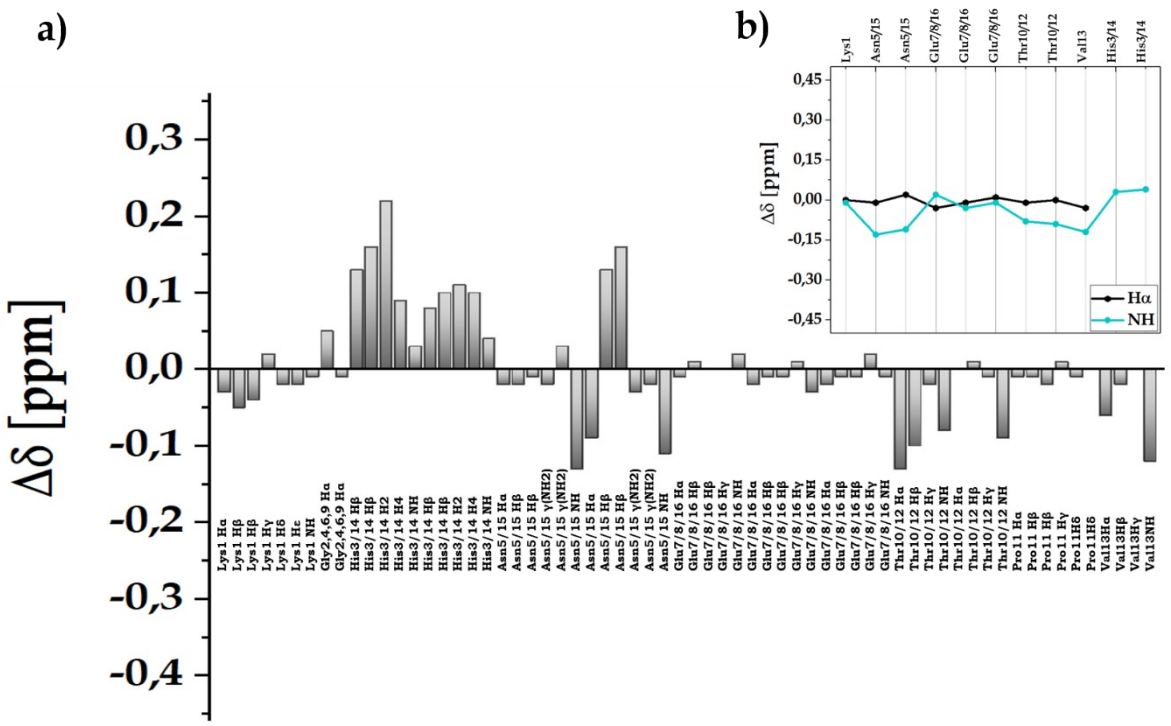


Fig. S9 The chemical shift variations provoked by the $Cu^{I}$ ions on the Fom2 protons. (a) A histogram presenting the measured changes in the values of the chemical shifts ($(\Delta\delta=\delta_{Fom2}-\delta_{Fom1\text{-}Cu2})$ for each amino acid residue. (b) A diagram presenting the chemical shift perturbations monitored for the signals of Hα i NH.

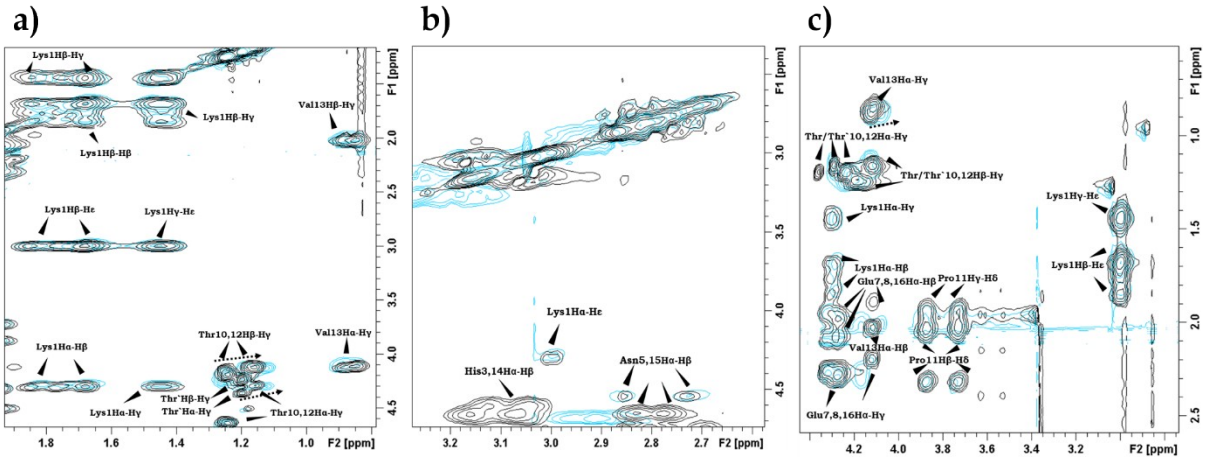


Fig. S10 (a), (b), (c) The $^{1}H$-$^{1}H$ TOCSY recorded for 4mM Fom2 before (black) and after (blue) the addition of 0.8 equivalents of $Cu^{I}$ ions with the chosen regions for aliphatic protons. The arrows indicate the most affected protons. The apostrophe indicate signals of the second Fom2 conformer. Conditions: pH≈ 7.40; 90%$H_2O$/10%$D_2O$, TSP 0.00 ppm.

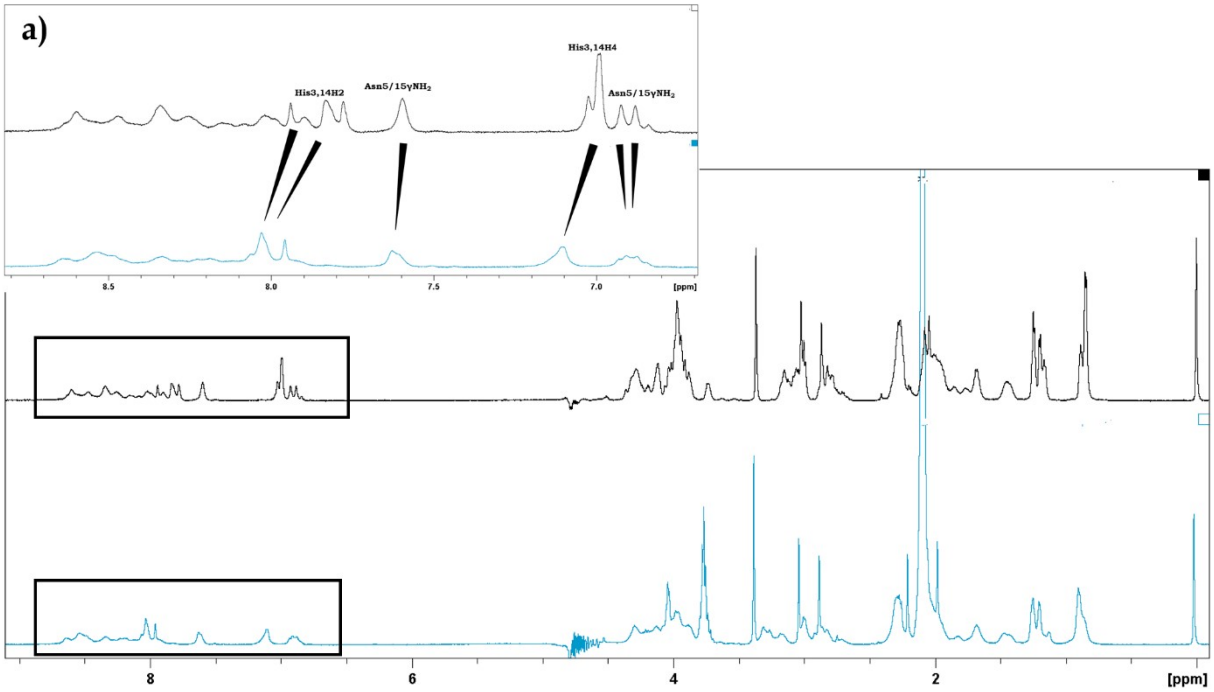


Fig. S11 The $^{1}$H-NMR spectra recorded for 4mM Fom2 before (top, black) and after (bottom, blue) the addition of 0.8 equivalents of $Cu^{I}$ ions. The top panel presents a selected region for the aromatic and amide protons. The arrows indicate the most affected protons. Conditions: pH≈ 7.40; 90%$H_2O$/10%$D_2O$,TSP 0.00 ppm. The sample of $Cu^{I}$ complex contained ≈0.5% of MeCN and 3.2 mM of HAsc.

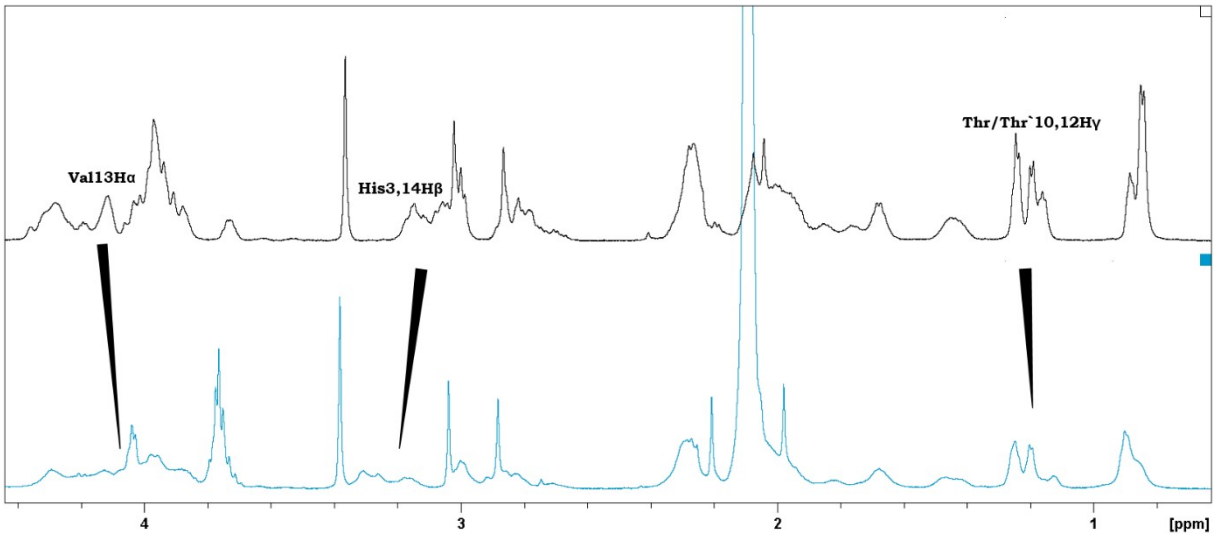


Fig. S12 The $^{1}$H-NMR spectra recorded for 4mM Fom1 before (top, black) and after (bottom, blue) the addition of 0.8 equivalents of $Cu^{I}$ ions with the chosen region for aliphatic protons. The arrows indicate the most affected protons. Conditions: pH≈ 7.40; 90%$H_2O$/10%$D_2O$, TSP 0.00 ppm. The sample of $Cu^{I}$ complex contained ≈0.5% of MeCN and 3.2 mM of HAsc.

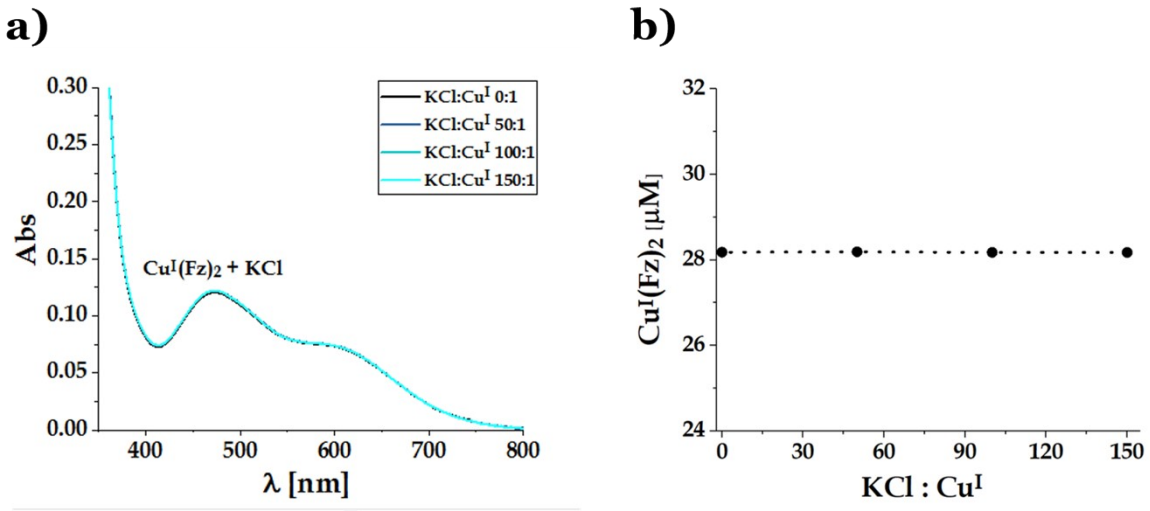


Fig. S13 (a) The UV-Vis absorption spectra of $[Cu^{I}(Fz)_2]^{3-}$ corresponding to the successive addition of portions of KCl. Conditions: ($[Cu^{I}]_{tot}$ ≈ 30 μM i $[Fz]_{tot}$ ≈ 70 μM; 100 mM bufor HEPES; pH= 7.40. (b) Titration curve corresponding to the successive addition of KCl into a $[Cu^{I}(Fz)_2]^{3-}$ solution; the concentration [μM] of $[Cu^{I}(Fz)_2]^{3-}$ was calculated based on the absorbance at $\lambda_{max}$= 470 nm.

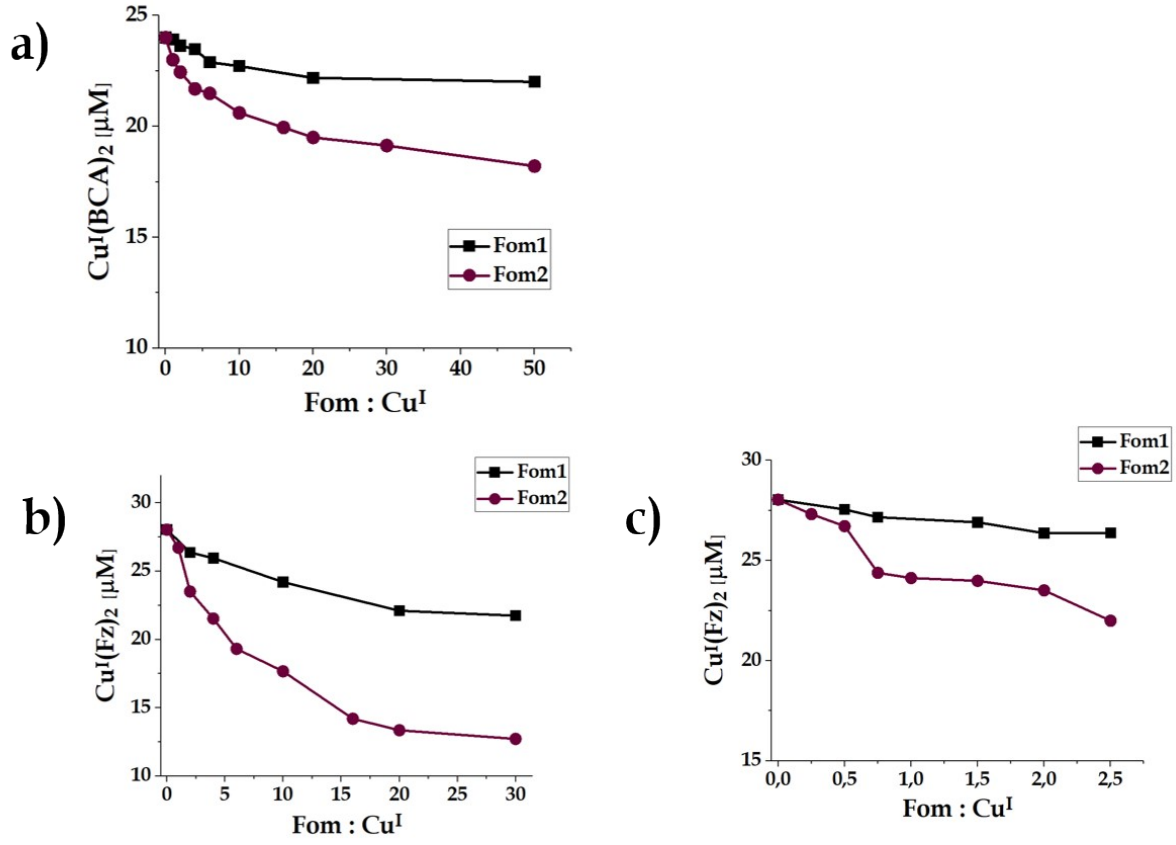


Fig. S14 Determination of $Cu^{I}$ dissociation constant $K_D$ based on the competitive titration with two spectroscopic probes $[Cu^{I}(BCA)_2]^{3-}$ and $[CuI(Fz)_2]^{3-}$ and two peptide ligands Fom1 and Fom2. (a) Variations of $[Cu^{I}(BCA)_2]^{3-}$ concentration [μM] in respond to different peptides:metal ion (Fom:$Cu^{I}$) molar ratio. (b) and (c) Variations of $[Cu^{I}(Fz)_2]^{3-}$ concentration [μM] in respond to different peptides:metal ion (Fom:$Cu^{I}$) molar ratio.

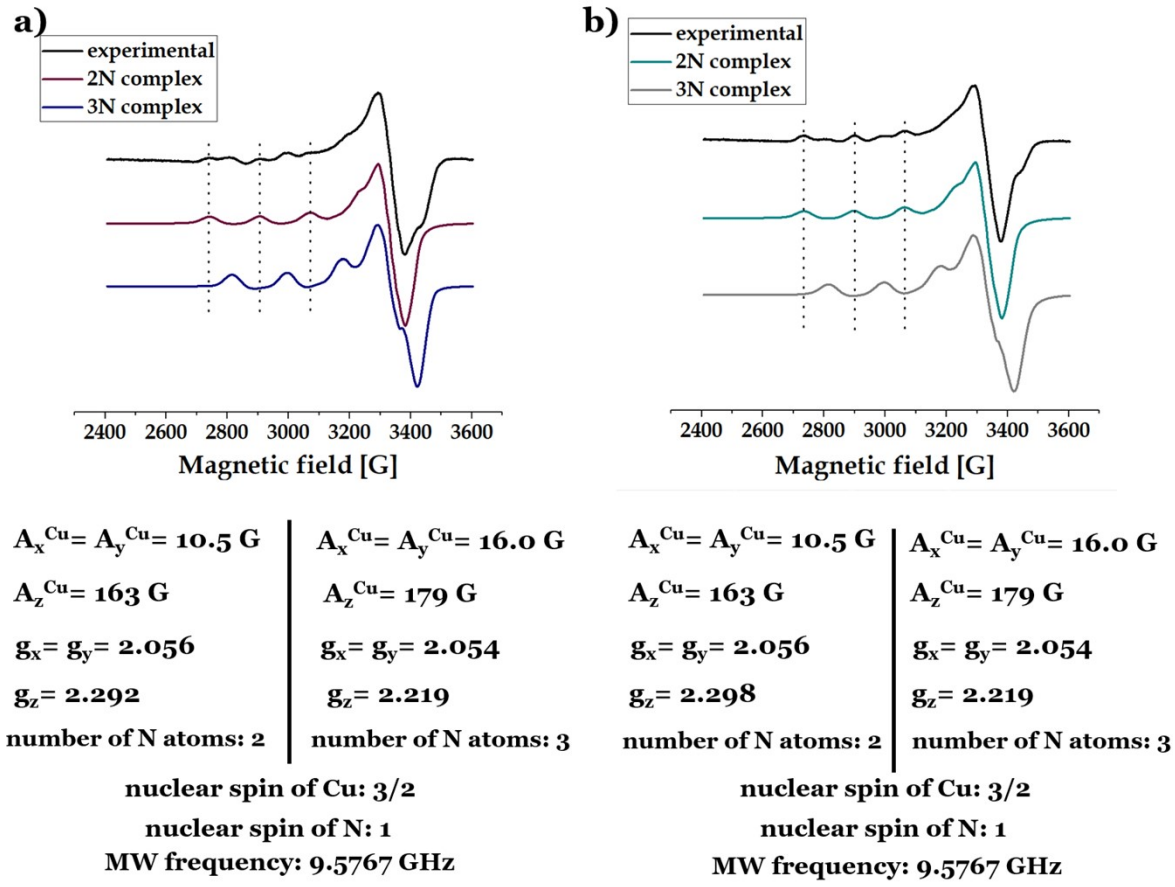


Fig. S15 The comparison of experimental X-band EPR spectra and simulated EPR spectra. (a) The EPR spectra recorded for the control sample of 1mM $Cu^{II}$-Fom1 complex. (b) The EPR spectra recorded for the air-oxidised sample of 1mM $Cu^{II}$-Fom2 complex. Spectra simulation and analysis of EPR parameters was carried out for both equilibrium $Cu^{II}$ complex species.

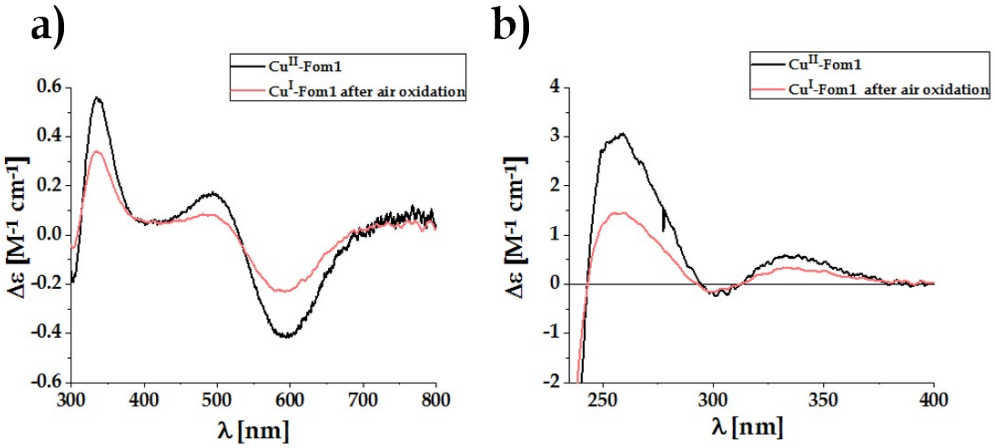


Fig. S16 The comparison of the CD spectra recorded for the control sample of 1mM $Cu^{II}$-Fom1 complex and for the air-oxidised sample of 1mM $Cu^{II}$-Fom1 complex. CD spectra recorded in (a) Vis and (b) UV regions. Conditions: pH= 7.40, ≈0.5% MeCN; [$Cu^{II}$] and [$Cu^{I}$] = 1 mM; molar ratio M:L 1:1.1.

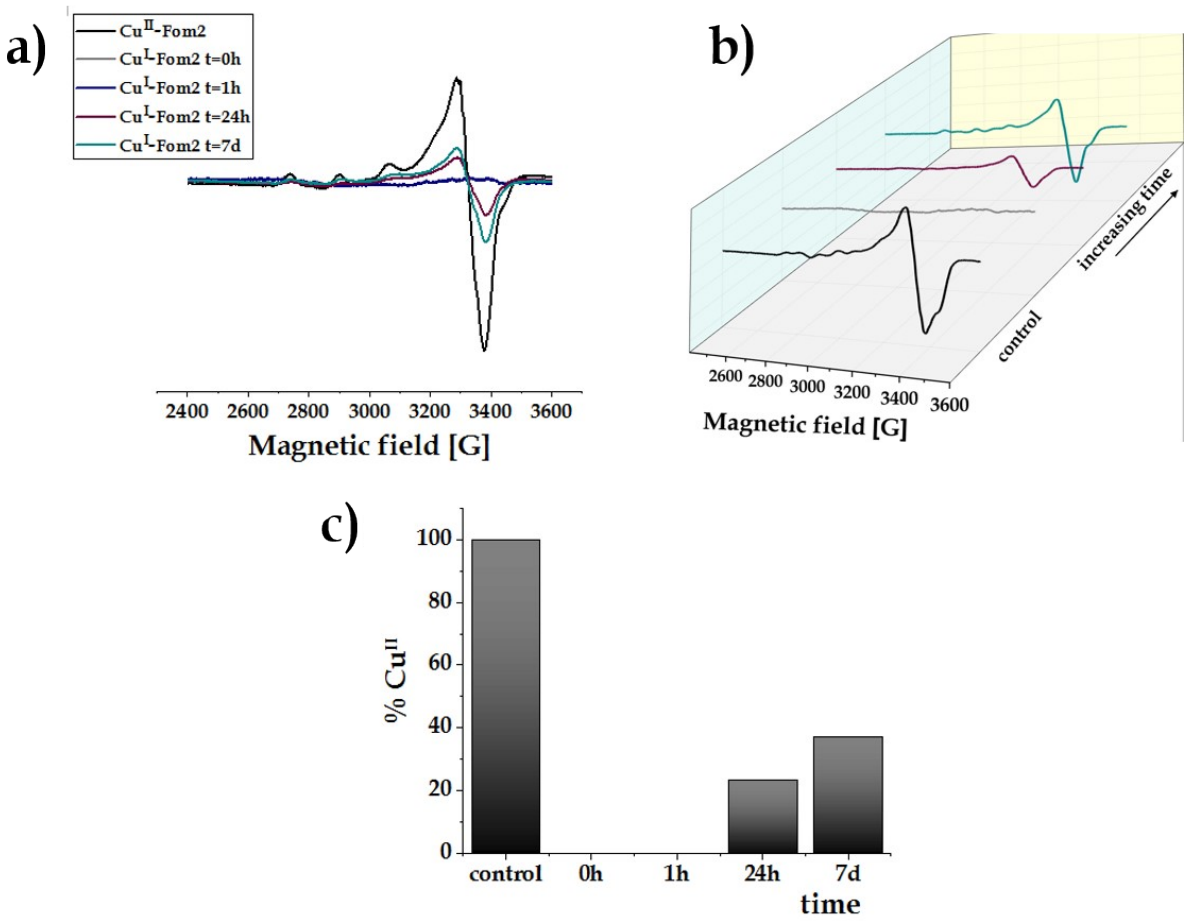


Fig. S17 Air-oxidation of 1mM Cu$^{I}$-Fom2 complex monitored by the X-band EPR. (a) 2D and (b) 3D plots presenting the time-dependent variations of EPR signals. (c) A histogram presenting % population of appearing Cu$^{II}$ complexes in the time-dependent mode. %Cu$^{II}$ were established from spectra quantification in reference to the control sample of 1mM Cu$^{II}$-Fom2. Conditions for air-oxidation: pH=7.40, 298K, $pO_2$≈20,3 kPa.

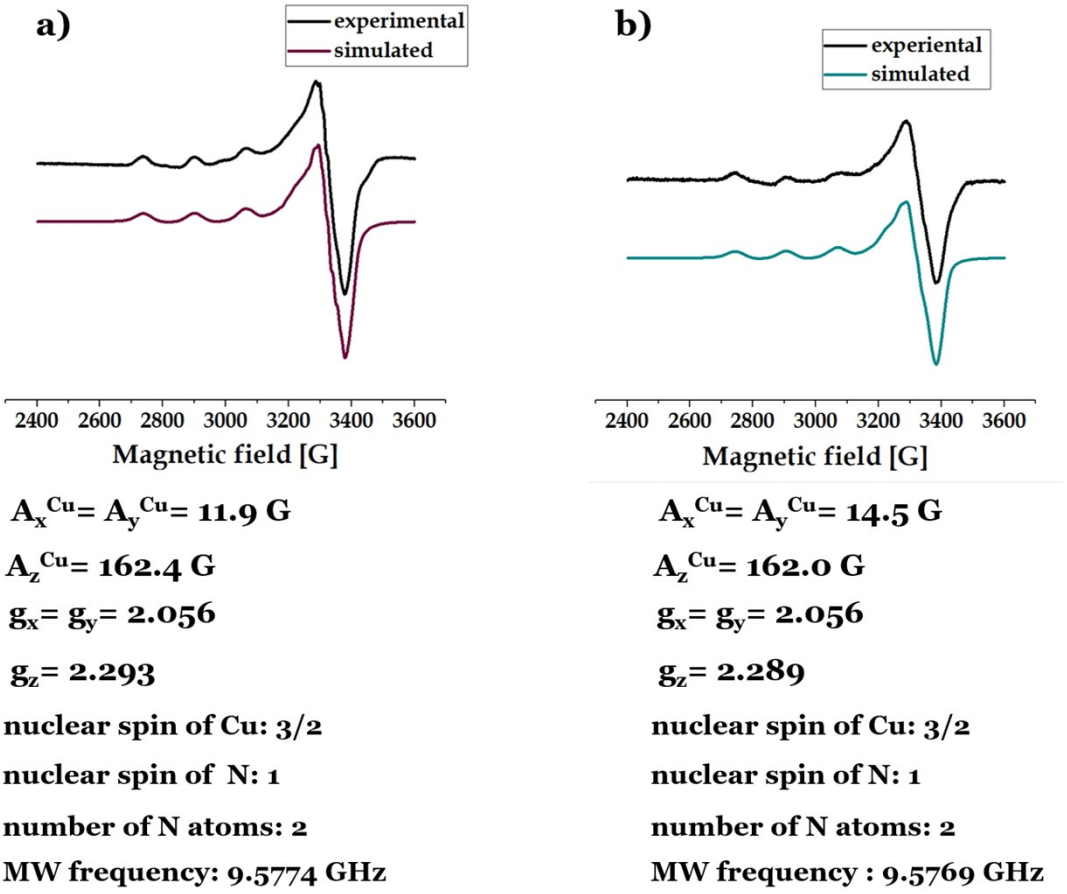


Fig. S18 The comparison of experimental X-band EPR spectra and simulated EPR spectra. (a) The EPR spectra recorded for the control sample of 1mM $Cu^{II}$-Fom2 complex. (b) The EPR spectra recorded for the air-oxidised sample of 1mM $Cu^{II}$-Fom2 complex.

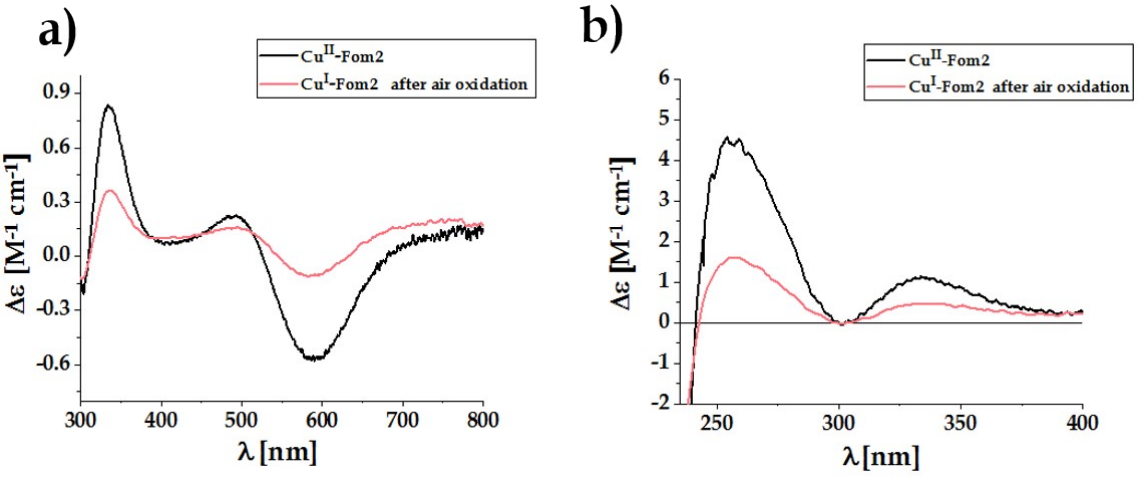


Fig. S19 The comparison of the CD spectra recorded for the control sample of 1mM $Cu^{II}$-Fom1 complex and for the air-oxidised sample of 1mM $Cu^{II}$-Fom1 complex. CD spectra recorded in (a) Vis and (b) UV regions. Conditions: pH= 7.40, ≈0.5% MeCN; [$Cu^{II}$] and [$Cu^{I}$] = 1 mM; molar ratio M:L 1:1.1.

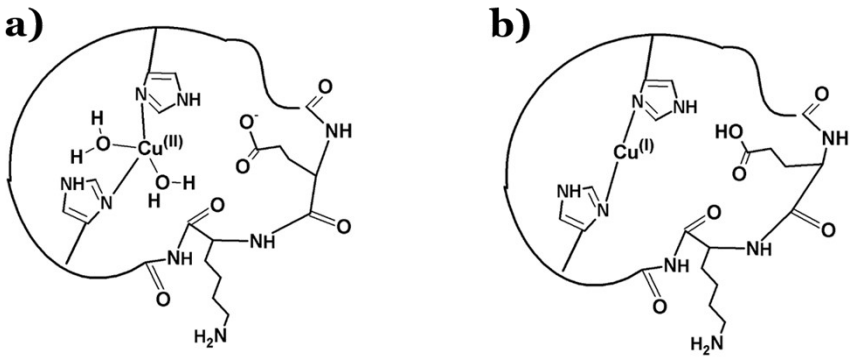


Fig. S20 (a) Schematic view on the structure of the $Cu^{II}$-Fom2 complex formed at pH=7.40; the coordination sphere was established based on the EPR, CD and UV-Vis spectra; (c) Schematic view on the metal ion binding site in $Cu^{I}$-Fom2 at pH=7.40 proposed from the NMR data.

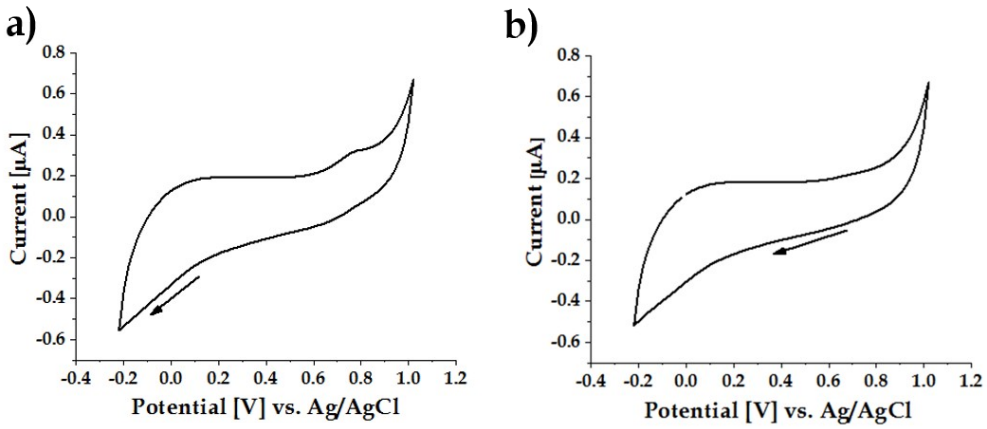


Fig. S21 The cyclic voltammograms recorded for (a) 1 mM Fom1 and (b) 1 mM Fom2 peptides at pH=7.40. Arrows indicate the direction of applied potential.

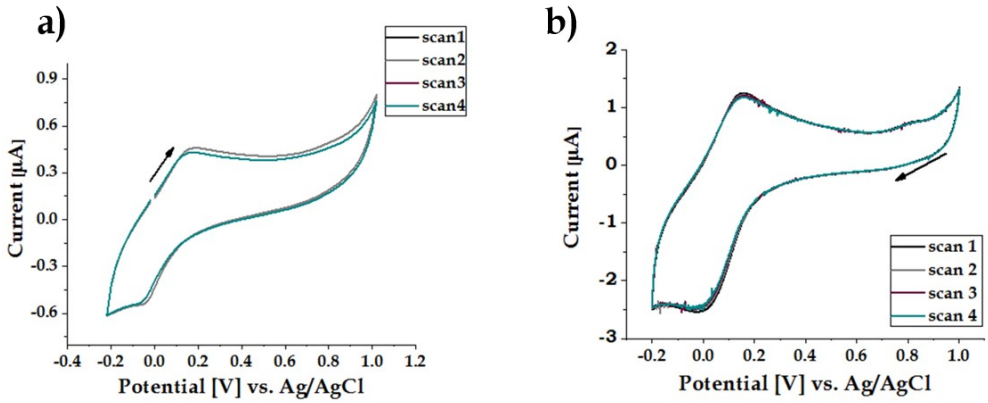


Fig. S22 The cyclic voltammograms recorded for (a) $Cu^{II}$-Fom1 and (b) $Cu^{I}$-Fom1 complexes at pH=7.40. Arrows indicate the direction of applied potential. Conditions: pH= 7.40; ≈0.5% MeCN; [$Cu^{II}$] and [$Cu^{I}$] = 0.5 mM; molar ratio M:L 1:2.

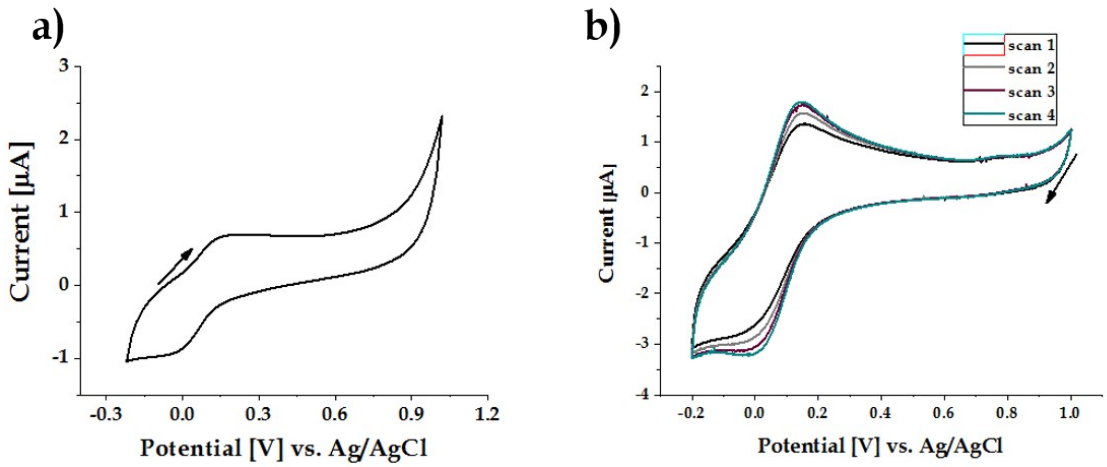


Fig. S23 The cyclic voltammograms recorded for (a) $Cu^{II}$-Fom2 and (b) $Cu^{I}$-Fom2 complexes at pH=7.40. Arrows indicate the direction of applied potential. Conditions: pH= 7.40; ≈0.5% MeCN; [$Cu^{II}$] and[$Cu^{I}$] = 0.5 mM; molar ratio M:L 1:2.

Table S3 The literature values of $E_{1/2}$ of different biological systems[1] and $E_{1/2}$ of copper complexs with Fom1 or Fom2 ligands (marked here as Fom).

| system | $E_{1/2}$ [V] vs. NHE |
|---|---|
| $O_2/H_2O_2$ | 0.295 |
| $Cu^{II}$-Aβ/$Cu^{I}$-Aβ | 0-0.400 |
| $Cu^{II}$-Fom/$Cu^{I}$-Fom | 0.270-0.300 |
| $Cu^{II}$-α-Syn/$Cu^{I}$-α-Syn | 0.241 |
| $Cu^{II}/Cu^{I}$ | ≈0.150 |
| DHA/HAsc | 0.078 |
| $O2/O2^{\bullet-}$ | -0.200 |
| GSSG/GSH | -0.228 |

[a] Aβ-amyloid-β; α-Syn- α-synuclein; DHA-dehydroxyascorbic acid; GSH-glutathione; GSSG- oxidized gluthatione

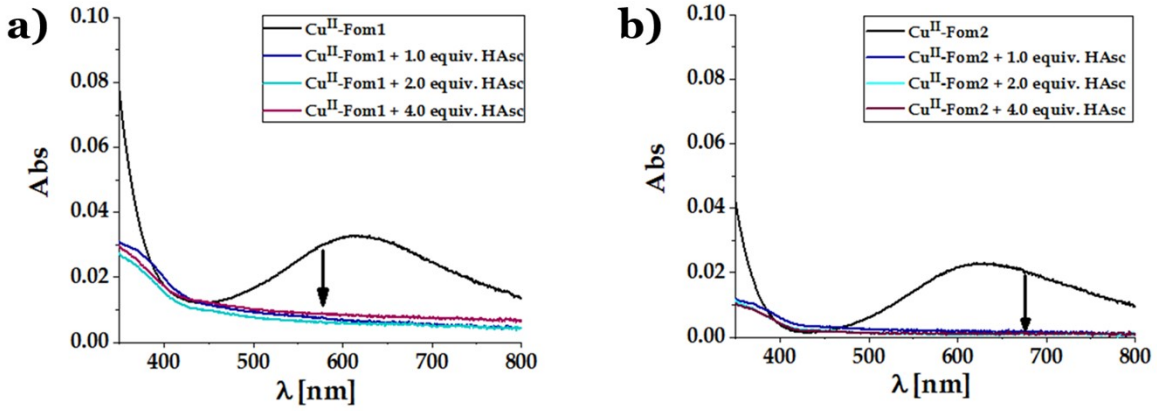


Fig. S24 The HAsc-induced reduction of (a) Cu$^{II}$-Fom1 and (b) Cu$^{II}$-Fom2 complexes monitored by the UV-Vis absorption spectra. Arrows indicate the decrease of absorption band upon addition of 0-4 equivalents of ascorbic acid. Conditions: pH= 7.40; pH was controlled before and after reduction; [Cu$^{II}$] = 1.0 mM; molar ratio M:L 1:1.1.

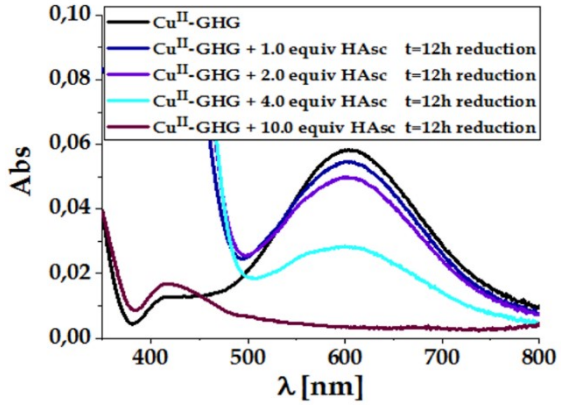


Fig. S25 The HAsc–induced reduction of Cu$^{II}$-GHG complex monitored by the UV-Vis absorption spectra. The reduction was initiated by the addition of 1,2,4 and 10 equivalents of ascorbic acid. Conditions: pH= 7.40; pH was controlled before and after

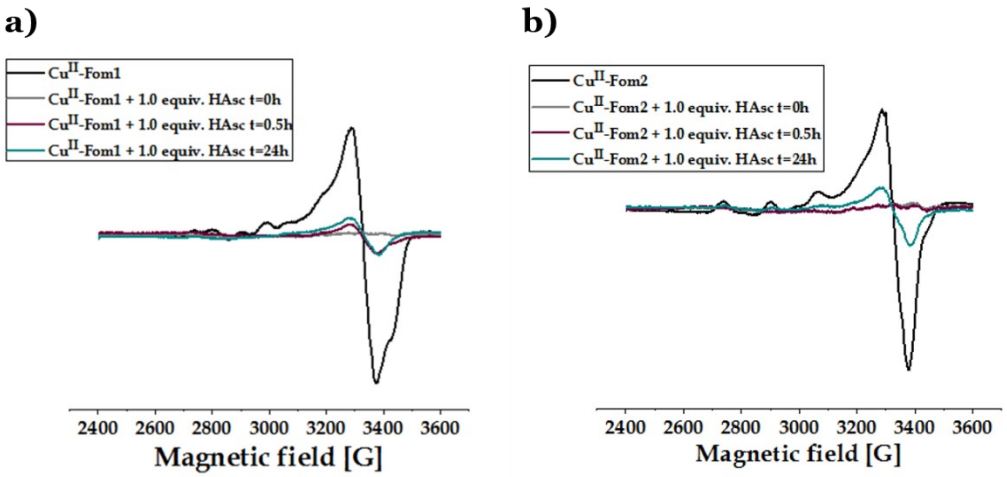


Fig. S26 The time-dependent re-oxidation of (a) Cu$^{I}$-Fom1 and (b) Cu$^{I}$-Fom2 complexes carried out in the presence of 1 equivalent of ascorbic acid and monitored by the X-band EPR. Spectra at t=0h presents the HAsc-induced reduction of Cu$^{II}$ complexes. Spectra at t=0.5h and t=24h were obtained for the air-induced re-oxidation. Conditions: pH= 7.40; pH was controlled before and after reduction; [Cu$^{II}$] = 1.0 mM (before reduction in the initial sample); molar ratio M:L 1:1.1. Conditions for air-oxidation: pH=7.40, 298K, $pO_2$≈20,3 kPa.

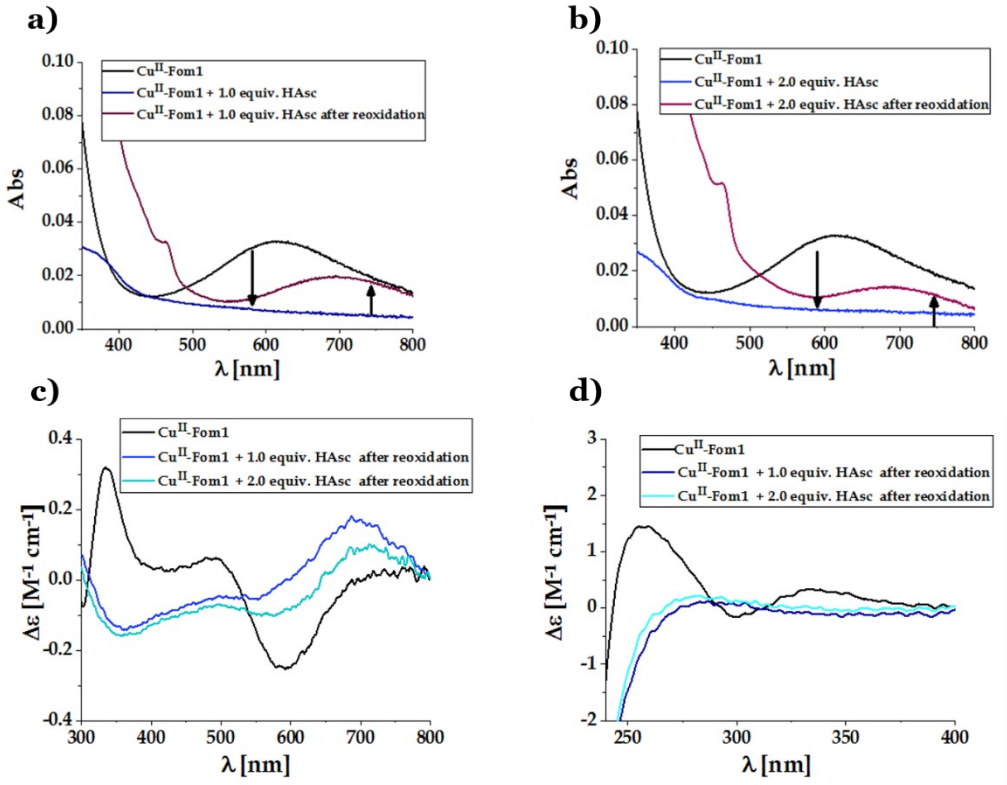


Fig. S27 The comparison of UV-Vis absorption spectra of Cu$^{II}$-Fom1 complex before and after HAsc-induced redox cycle. (a) HAsc-induced redox cycle of Cu$^{II}$-Fom1 provoked by the 1 equivalent of ascorbic acid. (b) HAsc-induced redox cycle of Cu$^{II}$-Fom1 provoked by the 2 equivalent of ascorbic acid.

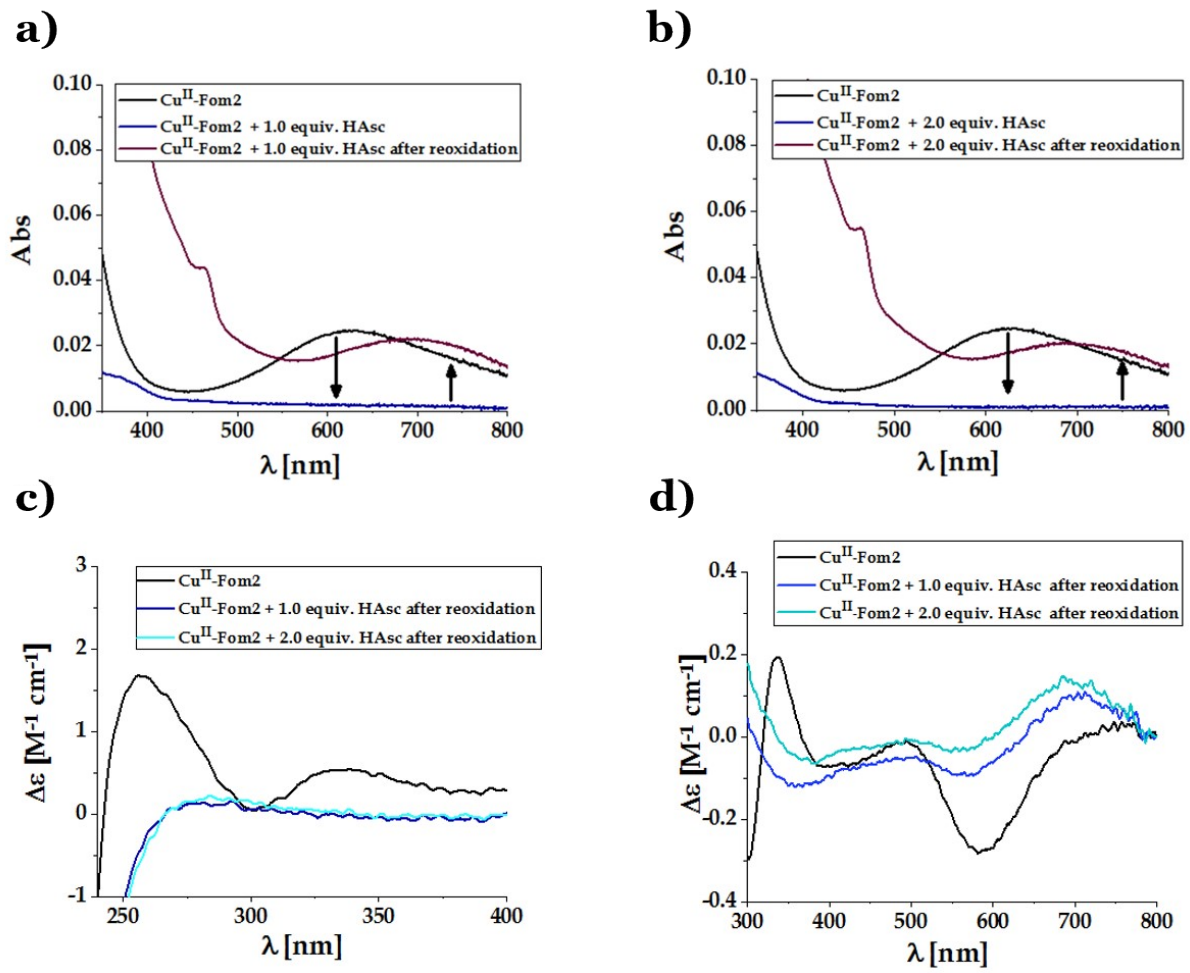


Fig. S28 The comparison of UV-Vis absorption spectra of $Cu^{II}$-Fom2 complex before and after HAsc-induced redox cycle. (a) HAsc-induced redox cycle of $Cu^{II}$-Fom2 provoked by the 1 equivalent of ascorbic acid. (b) HAsc-induced redox cycle of $Cu^{II}$-Fom2 provoked by the 2 equivalent of ascorbic acid. (c) and (d) HAsc-induced redox cycle of $Cu^{II}$-Fom2 monitored by the Vis and UV CD. Conditions: pH= 7.40; pH was controlled before and after reduction; [$Cu^{II}$] = 1.0 mM (before reduction in the initial sample); molar ratio M:L 1:1.1. Conditions for air-oxidation: pH=7.40, 298K, $pO_2$≈20,3 kPa.

**Ligands competition assays – the general idea and limitations**

The term "competitive titration" clarifies the general idea of this assay. At first, the solutions of two well-defined complexes $[Cu^{I}(BCA)_2]^{3-}$ and $[Cu^{I}(Fz)_2]^{3-}$ are obtained[2,3]. Both compounds exhibit distinct spectroscopic features, which allow tracking the whole experiments by UV-Vis spectroscopy. In the next step, a small and defined portion of investigated ligand (in our case Fom1 or Fom2) is added to a solution to provoke the competition. If the added compound exhibits a higher potential to bind $Cu^{I}$, the metal ion dissociates from $[Cu^{I}(BCA)_2]^{3-}$ or $[Cu^{I}(Fz)_2]^{3-}$ complex and coordinates to a stronger ligand. As the dissociation of $[Cu^{I}(BCA)_2]^{3-}$ and $[Cu^{I}(Fz)_2]^{3-}$ occurs, the intensities of their corresponding absorption

bands decrease. This decrease is proportional to the binding affinity and amount of the added ligand. The bigger portion of a high-affinity ligand is added, the higher decrease of absorption bands can be observed. Quantification of absorption spectra recorded during titration and competition can be then used for the calculation of a variety of thermodynamic constants (see the equations in Supplementary Materials). Since the ligand exchange is the key reaction during this experiment, the following assay can be considered as an indirect method for the determination of the binding affinity. Above all, this method is particularly useful for studying "spectroscopically-silent" systems like $Cu^{I}$-peptide complexes, for which the method of direct spectroscopic titration fails.

I applied two independent bidentate chelators, bicinchoninic acid (BCA) and ferrozine (Fz), as competitive ligands for $Cu^{I}$ [3–5]. Each of them binds $Cu^{I}$ quantitatively to yield a stable chromophoric 1:2 $[Cu^{I}(L)_2]^{3-}$ complexes with defined formation constants $\beta_2$ and distinct spectroscopic fingerprints. As it has been proposed by Xiao and Wedd[5] an excess of both BCA and Fz chelators provides the formation of 1:2 $[Cu^{I}(L)_2]^{3-}$ complexes and suppresses the presence of 1:1 $[Cu^{I}(L)]^{-}$ species. High concentration of $[Cu^{I}(L)]^{-}$ monomeric complexes compromises the reliable ligands competition and remains $K_D$ calculations invalid. Therefore, to ensure a dominant formation of $[Cu^{I}(L)_2]^{3-}$ with negligible contribution from $[Cu^{I}(L)]^{-}$ we used a 2.5 molar excess of BCA and Fz chelators.

At pH = 7.40 the high-affinity chelator BCA forms a stable $[Cu^{I}(BCA)_2]^{3-}$ complex which displays a strong absorbance at 358 nm ($\varepsilon$ = 42900 $M^{-1}$ $cm^{-1}$) and 562 nm ($\varepsilon$ = 7900 $M^{-1}$ $cm^{-1}$)[4]. Although two different formation constants ($\beta_2 = 10^{14.7}$ *versus* $\beta_2 = 10^{17.2}$) have been determined for $[Cu^{I}(BCA)_2]^{3-}$, mostly the value of $10^{17.2}$ has been considered as more reliable for quantitative analysis[5]. Xiao et al.[6] investigated that Fz binds $Cu^{I}$ significantly weaker forming $[Cu^{I}(Fz)_2]^{3-}$ chromophore with $\beta_2 = 10^{15.1}$ and two optical signatures at 470 nm ($\varepsilon$ = 4320 $M^{-1}$ $cm^{-1}$) and around 600 nm ($\varepsilon$~2450 $M^{-1}$ $cm^{-1}$). In this work, I employed these two distinct chelators (assigned henceforth as high- and low-affinity chelators) to provide a complementary analysis of $Cu^{I}$-peptide binding at respectively higher and lower metal-ion equilibrium limits[5].

For each competitive experiment, I used $[Cu^{I}(MeCN)_4]PF_6$ salt as a source of $Cu^{I}$ ions. Acetonitrile (MeCN) has been labeled as a week $Cu^{I}$ ligand with apparent affinities ranging from $\log\beta_1 = 2.63$, $\log\beta_2 = 1.39$ to $\log\beta_3 = 0.28$[7]. These values suggest that occurrence of pure $[Cu^{I}(MeCN)_4]^{+}$ and ternary ($Cu^{I}$ – MeCN-peptide or $Cu^{I}$ –MeCN-L] complexes was unlikely, especially after excessive addition of stronger ligands such as BCA or Fz. The extent to which MeCN may disturb quantification of competition equilibria was reported as 20 mM by Alies et al.[3]

All competitive experiments were performed in HEPES buffer, a member of the Good`s buffers family. To date, none of the studies have reported the ability of HEPES to bind $Cu^{I}$ ions[8]. Moreover, as in the previous case, in the presence of excess BCA or Fz the $Cu^{I}$-HEPES complexes are highly improbable to generate.

The meaningful quantitative analysis can be disturbed when $Cu^{I}$ ion coordinates simultaneously to both chelator and peptide ligands. So-called ternary complexes are divided into groups of stable and short-lived species[5,9]. The short-lived complexes are thermodynamically unstable intermediates, hence

any excess of ligands promotes their dissociation. By that, this group does not affect the competition equilibria. In contrast, the thermodynamically stable ternary species prevent ligand competition and restrict reliable quantification of the affinity of $Cu^I$ [5,9]. The formation of any ternary species changes the coordination environment of $Cu^I$ ion and yields new complexes with diverse electronic structures. That indeed changes the profile of recorded spectra and thus the presence of ternary species can be easily tracked by absorption spectroscopy.

All peptide ligands were used as chloride salts, which means that their addition to studied samples supplies a portion of week $Cl^-$ ligands. An investigation presented by Xiao et al. [6] revealed that the presence of $Cl^-$ was inadmissible mainly in experiments involving the low-affinity Fz chelator, due to decomposition of labile $[Cu^I(Fz)_2]^{3-}$ complex. According to the mentioned studies the dissociation of $[Cu^I(Fz)_2]^{3-}$ was facilitated mainly above 2 mM concentration of $Cl^-$. Nevertheless, I decided to examine the tendency of $[Cu^I(Fz)_2]^{3-}$ to decompose in the presence of chloride anions under conditions applied in my competitive studies. The results of $[Cu^I(Fz)_2]^{3-}$ titration by the extent of even 150 equivalents of KCl are shown in Figure S13. It is apparent from these data that none of the portions of KCl causes dissociation of $[Cu^I(Fz)_2]^{3-}$ complex. Based on that I ensured the lack of interference of chloride anions in equilibria investigated during the course of my competitive assays.

Competitive titration equilibria: L ($Cu^I$ chelator, BCA or Fz), P (peptide ligand); $K_{ex}$ – ligand exchange reaction constant

$$Cu^IP + 2L \rightleftarrows Cu^IL_2 + P \qquad K_{ex} = \frac{[Cu^IL_2][P]}{[Cu^IP][L]^2} \qquad (1)$$

Formation equilibrium for $Cu^I$ complexes with BCA and Fz chelators (marked as L); $\beta_2$ – complex formation constant

$$Cu^I + 2L \rightleftarrows Cu^IL_2 \qquad \beta_2 = \frac{[Cu^IL_2]}{[Cu^I][L]^2} \qquad (2)$$

Dissociation equilibrium for $Cu^I$ complexes with peptide ligands, $K_D$ – $Cu^IP$ complex dissociation constant

$$Cu^IP \rightleftarrows Cu^I + P \qquad K_D = \frac{[Cu^I][P]}{[Cu^IP]} \qquad (3)$$

The relationship between equilibria

$$\frac{[P]}{[Cu^{I}P]} = \frac{K_D}{[Cu^{I}]} \qquad \frac{[Cu^{I}L_2]}{[L]^2} = \beta_2\,[Cu^{I}] \qquad K_{ex} = K_D\,\beta_2 \tag{4}$$

Equilibrium concentrations of *[Cu$^{I}$P], [P], [L]* and total concentration of *[Cu$^{I}$]$_{tot}$, [P]$_{tot}$, [L]$_{tot}$*

$$[Cu^{I}P] = [Cu^{I}]_{tot} - [Cu^{I}L_2] \tag{5}$$

$$[P] = [P]_{tot} - [Cu^{I}P] \tag{6}$$

$$[L] = [L]_{tot} - 2[Cu^{I}L_2] \tag{7}$$

Total concentration of peptide ligand *[P]$_{tot}$* considering all reactions occurring during the competitive titration

$$[P]_{tot} = [P] + [Cu^{I}P] \tag{8}$$

$$[P]_{tot} = \frac{K_D\,[Cu^{I}P]}{[Cu^{I}]} + [Cu^{I}P] \tag{9}$$

$$K_D\,\beta_2 = K_{ex} = \frac{[Cu^{I}L_2][P]}{[Cu^{I}P][L]^2} \tag{10}$$

$$[P]_{tot} = \frac{K_D\,\beta_2[Cu^{I}P][L]^2}{[Cu^{I}L_2]} + [Cu^{I}P] \tag{11}$$

$$[P]_{tot} = \frac{K_D\,\beta_2[Cu^{I}P]}{[Cu^{I}L_2]}\frac{[L]^2}{[Cu^{I}L_2]} + [Cu^{I}P] \tag{12}$$

Total concentration of Cu$^{I}$ ions *[Cu$^{I}$]$_{tot}$* considering all reactions occurring during the competitive titration

$$[Cu^{I}]_{tot} = [Cu^{I}P] + [Cu^{I}L_2] \tag{13}$$

$$\frac{[Cu^{I}P]}{[Cu^{I}]_{tot}} = \frac{[Cu^{I}]_{tot}}{[Cu^{I}]_{tot}} - \frac{[Cu^{I}L_2]}{[Cu^{I}]_{tot}} = 1 - \frac{[Cu^{I}L_2]}{[Cu^{I}]_{tot}} \quad (14)$$

Total concentration ratio $[P]_{tot}/[Cu^{I}]_{tot}$ considering all reactions occurring during the competitive titration

$$\frac{[P]_{tot}}{[Cu^{I}]_{tot}} = \frac{\frac{K_D\,\beta_2[Cu^{I}P]}{[Cu^{I}L_2]}\frac{[L]^2}{[Cu^{I}L_2]} + [Cu^{I}P]}{[Cu^{I}]_{tot}}$$

adding an equation (14)

$$\frac{[P]_{tot}}{[Cu^{I}]_{tot}} = (1 - \frac{[Cu^{I}L_2]}{[Cu^{I}]_{tot}})\frac{K_D\,\beta_2[L]^2}{[Cu^{I}L_2]} + (1 - \frac{[Cu^{I}L_2]}{[Cu^{I}]_{tot}})$$

adding an equation (7)

$$\frac{[L]^2}{[Cu^{I}L_2]} = \frac{[[L]_{tot} - 2[Cu^{I}L_2]]^2}{[Cu^{I}L_2]} = (\frac{[L]_{tot}}{[Cu^{I}L_2]} - 2)^2[Cu^{I}L_2]$$

The final equation for the calculation of values of $K_D$–$Cu^{I}P$ complex dissociation constant

$$\frac{[P]_{tot}}{[Cu^{I}]_{tot}} = (1 - \frac{[Cu^{I}L_2]}{[Cu^{I}]_{tot}})K_D\,\beta_2 + (\frac{[L]_{tot}}{[Cu^{I}L_2]} - 2)^2[Cu^{I}L_2] + (1 - \frac{[Cu^{I}L_2]}{[Cu^{I}]_{tot}})$$


1 C. Wang, L. Liu, L. Zhang, Y. Peng and F. Zhou, *Biochemistry*, 2010, 8134–8142.

2 I. Zawisza, M. Rózga and W. Bal, *Coord. Chem. Rev.*, 2012, **256**, 2297–2307.

3 B. Alies, B. Badei, P. Faller and C. Hureau, *Chem. A Eur. J.*, 2012, 1161–1167.

4 D. Kahra, M. Kovermann and P. Wittung-Stafshede, *Biophys. J.*, 2016, **110**, 95–102.

5 Z. Xiao and A. G. Wedd, *Nat. Prod. Rep.*, 2010, 768–789.

6 Z. Xiao, L. Gottschlich, R. Van Der Meulen, S. R. Udagedara and A. G. Wedd, *Metallomics*, 2013, 501–513.

7 K. L. Haas, A. B. Putterman, D. R. White, D. J. Thiele and K. J. Franz, *J. Am. Chem. Soc.*, 2011, **133**, 4427–4437.

8 C. M. H. Ferreira, I. S. S. Pinto, E. V. Soares and H. M. V. M. Soares, *RSC Adv.*, 2015, **5**, 30989–31003.

9 T. R. Young, A. G. Wedd and Z. Xiao, *Metallomics*, 2017, **10**, 108–119.